
Article:
Smyl, D. orcid.org/0000-0002-6730-5277 and Liu, D. (2019) Damage tomography as a state estimation problem : crack detection using conductive area sensors. IEEE Sensors Letters.

https://doi.org/10.1109/lsens.2019.2940748

Damage tomography as a state estimation problem: crack detection using conductive area sensors

Danny Smyl[1] and Dong Liu[2]

[1]*Department of Civil and Structural Engineering, University of Sheffield, Sheffield, UK*
[2]*Hefei National Laboratory for Physical Sciences at the Microscale and Department of Modern Physics, University of Science and Technology of China, Hefei 230026, China*

Abstract—Typically, structural damage tomography (SDT) approaches aim to reconstruct a parameter field containing damage information from distributed data by solving an iterative inverse problem. Often, there are two shortcomings in adopting such an approach: (a) the high computational expense and (b) temporal information is inadequately used. In principle, both issues may be alleviated by approaching SDT as a state-estimation problem – i.e. treating the reconstruction problem as a temporally-evolving stochastic process. In this letter, we study the feasibility of state estimates in SDT. For this, we use an extended Kalman filter (EKF) for electrical resistance tomography (ERT) imaging of progressive cracking on an experimentally-tested reinforced concrete beam with an applied surface area sensing skin. In the investigation, we quantitatively analyze the effect of including multiple temporal data sets and corroborate EKF-ERT reconstructions with standard and advanced ERT approaches. It is shown that increasing the amount of temporal data significantly improves the quality of EKF-ERT reconstructions, which compare favorably with the standard and advanced ERT approaches. In addition, for the data sets used herein, the EKF-ERT regime computed seven reconstructions approximately 50-100 times faster than the standard and stacked approaches required to reconstruct one image, respectively.

Index Terms—Extended Kalman filter, inverse problems, state estimation, structural health monitoring

I. INTRODUCTION

Structural damage tomography (SDT) is an emerging field where users aim to image structural damage processes. Specifically, in SDT users aim to estimate a particular two- or three-dimensional parameter field using distributed measurements – usually by solving an inverse problem [1]. In turn, by interpreting the reconstructions, an assessment of structural damage can be made. Possibly owing to improvements in computational resources and advances in inverse methodologies, SDT has become the source of much research interest in recent years [2], [3]. In general, SDT involves estimating (reconstructing) a parameter field θ from noisy distributed data d. In doing this, one generally aims to minimize a functional of the form

$$\Psi = ||d - U(\theta)||^2 + R(\theta) \tag{1}$$

where $||\cdot||$ is the L_2 norm, U is a numerical model for the problem's physics, and R is a regularization term which stabilizes the inversion processes since many SDT problems are non-linear and ill-posed [2]. Some contemporary examples of SDT include digital image correlation [4], electrical resistance tomography (ERT) [5], and acoustic tomography [6]. To improve the resolution of SDT images, the use of iterative methods is commonly used. Unfortunately, the computational expense of iterative SDT problems can be staggering and scales exponentially with the degrees of freedom in the inverse problem. Moreover, many SDT inversion regimes often do not incorporate sufficient information available in previous data sets. This issue has been addressed in previous ERT-relevant works; e.g. researchers have reduced ill-conditioning by incorporating information on known conductivity changes into the underlying inverse problem [7] and improved reconstructions by including information related to the mechanical deformation [8].

In this work, we may approach the SDT problem as a state estimation problem. In state estimation problems, we treat the reconstruction of θ as a temporally-varying stochastic process. The use of state estimation is commonly adopted in reconstruction problems where the dynamic evolution of the process of interest is extremely fast – often making conventional inverse regimes infeasible for online monitoring [9]. Some examples of the former include process tomography [10] and motion tracking [11]. While there are numerous regimes available for state estimation [12], [13], the extended Kalman filter (EKF) has proven to be robust and broadly applicable over the years [14]–[17], and is adopted herein for SDT imaging.

In this letter, we aim to determine the feasibility of using state estimation for SDT in order to (a) decrease computational costs and (b) incorporate information available from prior data sets into SDT reconstructions. Moreover, while other work in the area of structural health monitoring has used Kalman filters to identify damage/structural parameters (e.g. [18]–[20]), the novelty of this work lies in the use of state estimation for 2D *spatial* damage detection. For this, we begin by applying an EKF to a modern SDT modality: ERT*. Following, we test the EKF–ERT regime using experimental data where we aim to image progressive cracking on a reinforced concrete beam. Lastly, concluding remarks are provided.

II. EKF–ERT REGIME FOR DAMAGE TOMOGRAPHY

Using ERT, we aim to determine the electrical conductivity distribution σ from boundary voltage measurements V and knowledge of an electric current stimulation pattern. Usually, the solution to the ERT inverse problem is obtained by minimizing a functional similar

Corresponding authors: D. Smyl (d.smyl@sheffield.ac.uk) and Dong Liu (dong2016@ustc.edu.cn).

Digital Object Identifier 10.1109/LSENS.2017.0000000

*While other modalities are certainly applicable candidates for crack imaging with an EKF, ERT is primarily selected because it is well suited for reconstructing cracks of varying complexity (a common target in SDT) [5].

to the one in Eq. 1. However, in the EKF-based state estimation approach to ERT, we use a problem description similar to that in [21] where the temporal evolution at step $k+1$ of σ_{k+1} is given by

$$\sigma_{k+1} = F_k \sigma_k + w_k \tag{2}$$

where $F_k = I$ is the random-walk state transition matrix, I is the identity matrix, and w_k is the white process noise with a corresponding covariance matrix Γ^w that controls the rate of change of σ. Γ^w is also known as the process matrix and is computed using $\Gamma^w = s^2 I$ where s is the standard deviation of the process transition. It is important to remark that Γ^w encodes prior information into the evolution of σ. Therefore, selecting a statistically accurate description of Γ^w is expected to improve damage estimates. For the purposes of this work, $s = 0.1$ provided a reasonably robust first-order approximation.

Having broadly defined the process's temporal evolution, we may now write down the observation model at step k

$$V_k = U_k(\sigma_k) + v_k \tag{3}$$

where U_k is the ERT finite element forward model adopting the complete electrode model described in [22], [23], V_k is the measurement at step k, and v_k is the Gaussian measurement noise with corresponding covariance matrix Γ^v. We may now linearize the model in Eq. 3 about the current predicted state $\sigma_{k|k-1}$ by writing

$$V_k = U_k(\sigma_{k|k-1}) + J_k(\sigma_k - \sigma_{k|k-1}) + v_k \tag{4}$$

where $J_k = \frac{\partial U_k}{\partial \sigma_k}|_{\sigma_{k|k-1}}$ is the Jacobian, also referred to as the sensitivity matrix. Following, we define the pseudo measurement y_k as

$$y_k = V_k - U_k(\sigma_{k|k-1}) + J_k \sigma_{k|k-1} \approx J_k \sigma_k + v_k \tag{5}$$

where the right hand side is the linearized form the observation equation used herein. Bearing in mind that we have assumed the noise is Gaussian and the observation equation is linear: the Kalman filter estimate of σ_k on the basis of all measurements taken until state k, the EKF-ERT estimate minimizes the following functional

$$\Psi_k = ||\sigma_k - \sigma_{k|k-1}||^2_{C^{-1}_{k|k-1}} + ||y_k - J_k \sigma_k||^2_{(\Gamma^v_k)^{-1}} + \alpha ||R(\sigma_k - \sigma_{\exp})||^2 \tag{6}$$

where $C_{k|k-1}$ is a covariance matrix updated at each step, $\sigma_{\exp}$ is the expected value of σ, R is a regularization matrix, and α is a regularization parameter. The inclusion of regularization in this regime is owed to the ill-posed nature of ERT. Inasmuch, α and R encode prior information in the solution and may be determined statistically or empirically [24], [25]. Here, R=I and α=6.9×10^{-4} was selected using a standard L-curve analysis using 8 points. Moreover, $\sigma_{\exp}$=argmin$\{||V_{\text{undamaged}} - U(\sigma_{\text{homogeneous}})||^2\}$ was computed using the best homogeneous estimate of σ with data from the undamaged state.

Now, by defining the augmented pseudo-measurement matrix $\bar{y}_k$ = Blkdiag$[y_k, \sqrt{\alpha} R \sigma_{\exp}]$. and the measurement matrix H_k = Blkdiag$[J_k, \sqrt{\alpha} R]$ we may concisely rewrite the cost functional as

$$\Psi_k = ||\sigma_k - \sigma_{k|k-1}||^2_{C^{-1}_{k|k-1}} + ||\bar{y}_k - H_k \sigma_k||^2_{(\Gamma_k)^{-1}} \tag{7}$$

where Γ_k is a block diagonal matrix written as Γ_k = Blkdiag$[\Gamma^v_k, I]^{\mathrm{T}}$. Now, for clarity, we summarize the EKF-ERT regime as follows:

- *Initialize* – $\sigma_{0|0} = \sigma_{\exp}$, $C_{0|0} = \Gamma^w$
- *Measurement updating* – i.e. filtering
  - Compute the Kalman gain, $G_k = C_{k|k-1} H_k^{\mathrm{T}} (H_k C_{k|k-1} H_k^{\mathrm{T}} + \Gamma_k)^{-1}$
  - Update the covariance estimate $C_{k|k} = (I - G_k H_k) C_{k|k-1}$
  - Update the state estimate $\sigma_{k|k} = \sigma_{k|k-1} + G_k(\bar{y}_k - H_k \sigma_{k|k-1})$.
- *Prediction* – i.e. moving the estimate and its covariance in time
  - Compute $C_{k+1|k} = F_k C_{k|k} F_k^{\mathrm{T}} + \Gamma^w$
  - Compute $\sigma_{k+1|k} = F_k \sigma_{k|k}$
- Project $\sigma_{k+1} < 0$ to 10^{-5} to ensure real U solutions.

From an implementation standpoint, it is important to recall that the ERT-EKF regime presented here is not iterative in the "traditional" optimization sense. In other words, one set of data is not iterated on until some convergence criteria is met. Rather, each state estimate (conductivity estimate) is computed once for a given data set, and then updated upon evaluation of the next data set.

III. STATE ESTIMATION OF PROGRESSIVE DAMAGE ON A CONCRETE BEAM

A. Experimental program and numerical preliminaries

In this section we aim to determine the feasibility of treating damage tomography as a state estimation problem. To investigate this query, we apply the EKF described in the previous section to ERT imaging of a lightly reinforced concrete beam with an applied silver sensing skin. In the testing regime, thoroughly detailed in [1], [5], a 15.2×50.8×15.2 cm beam was loaded in three-point bending with a maximum load of approximately 120 kN. On the beam's surface, a sensing skin with 28 copper boundary electrodes was utilized in the ERT experimental program. In the program, a total of 54 1.0 mA DC injections were applied between electrodes i and j, $i = 6, 21$ and $j = 1, ..., 28, i \neq j$. For each injection, 1458 adjacent electrode potentials were measured. Moreover, a total of 8 usable ERT measurements were taken at the following loading increments: 0, 2.2, 18.2, 29.8, 39.1, 71.2, and 85 kN (two reference measurement were logged at 0 kN). We would like to mention that the sensing skin, manually painted on the broad surface of the beam, had an electrical conductivity over two orders of magnitude larger than the contacted concrete. As such, we assume herein that the current leakage into the beam is negligible. For reference, an image of the cracked sensing skin (39.1 kN) with numbered electrodes is shown in Fig. 1a.

In solving the state estimation problem, we used a finite element discretization with $N_{\mathrm{e}} = 9680$ quadratic triangular elements and $N_n = 5047$ nodes for solving the forward problem. For computing the Jacobians, a semi-analytical method outlined in [26] was used. The EKF was implemented using a MATLAB script using the parameters defined in the previous section and a noise covariance matrix (Γ^v) computed using diagonal matrix entries corresponding to 2% standard deviation of the measurement magnitudes. In the following subsection, the EKF-ERT damage tomography regime will be evaluated.

B. EKF-ERT imaging

In this subsection, we test the EKF-ERT regime's feasibility to image progressive cracks denoted Damage Level 1 – Damage Level 6. To do this, we execute the regime using between $k = 3$ and $k = 7$ data sets – this does not include reference data set 1, which is used herein for computing $\sigma_{\exp}$. In the first suite of reconstructions, where $k = 3$, we aim to reconstruct the highest levels of damage, corresponding to Damage Levels 4 – 6. In the final suite of reconstruction, where $k = 7$

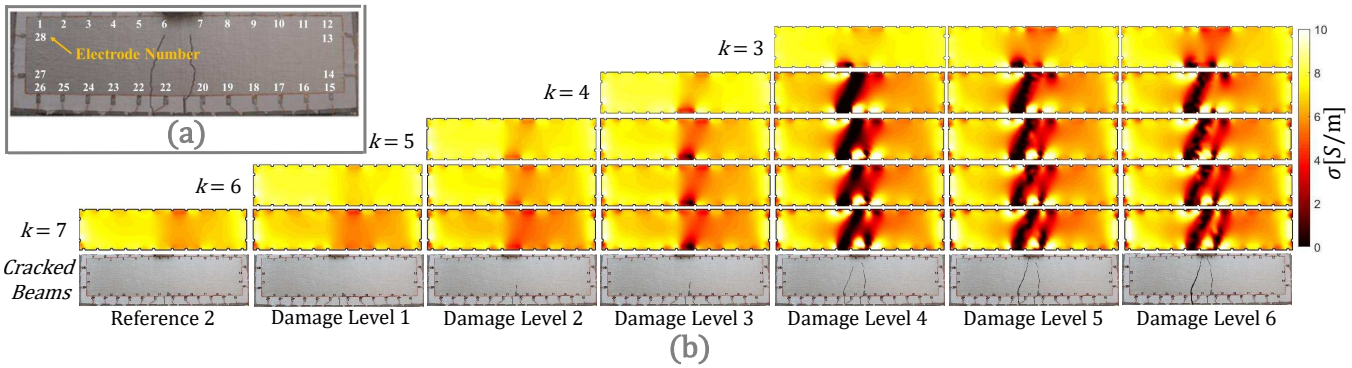

Fig. 1. Images showing (a) photo of a cracked sensing skin with numbered electrodes atop a reinforced concrete beam subjected to three-point bending and (b) state estimations of progressive damage using an EKF applied to ERT. The values of k ranging from 3 to 7 (top to bottom) denote the total number of data sets used. The levels of damage range from zero in the reference case (far left) to the maximum level (far right).

we use all data sets including reference data set 2. The reconstructions for $k = 3$ to $k = 7$ are provided in Fig. 1b.

The images shown in Fig. 1 support the feasibility of treating damage tomography as a state estimation problem as the majority of the cracks were captured via localized reductions in σ. As an obvious extension, the results also generally support the use of the EKF-ERT regime for imaging progressive damage – at least when there is sufficient temporal data. Indeed, the EKF reconstructions satisfactorially localized the cracks for Damage Levels 3 - 6 and $k > 3$. However, when there was insufficient prior data ($k < 3$) the damage was poorly localized. This results from the fact that the change in state between the reference state and Damage Level 4 was sufficiently large to violate the linearization assumption in Eq. 5. On the other hand, for the case where $k = 4$, the added data set corresponding to Damage Level 3 was adequate to visually localize the prominent left-hand crack present at Damage Level 4.

There are two additional, yet subtle, realizations that can be made from Fig. 1b, namely (i) the crack present at Damage Level 2 is invisible in all cases and (ii) the added data between cases ranging from $k = 5$ to $k = 7$ did not significantly increase reconstruction quality. Regarding comment (i), the crack present in in Damage Level 2 is likely invisible in ERT images due to (a) the indistinguishability of data with respect to the reference data , i.e. $||V_{k=2} - V_{k=1}|| < \varepsilon$ where ε is a measurement precision term and (b) the selection of the process matrix Γ^w, while sufficient for higher levels of damage, likely utilized an excessively large process standard deviation s. In practice, one may address (a) and (b) by, e.g., optimizing electrode locations to increase sensitivity or optimizing Γ^w. Regarding comment (ii), the blurriness in images for Damage Levels 4 – 6 largely results from the massive change in state from Damage Level 3 to Damage Level 4. The large change has a residual effect on the successive images that cannot be adequately compensated based on such low temporal resolution data. In future work, this problem may be alleviated by increasing the measuring frequency, improving the prior model using a more physically realistic regularization approach (i.e. using Total Variation or L_1 regularizers for R) coupled with iterative optimization, or using proxy data sets between large data state changes (executing the same data set several times so the EKF regime can "catch up").

As a whole, we would like to mention that the EKF-ERT crack reconstructions using only a few data sets likely have lower resolution than those in previous works utilizing stacking, model-error estimation, and advanced regularization methods. To investigate this, we compare EKF reconstructions to (a) an estimate obtained using a positively constrained standard iterative approach equipped with a TV regularizer and (b) a stacked approach. For the stacked approach (details in [1]), we use a smoothness prior in computing the (non-cracked) background conductivity σ_1 and TV for the change in conductivity ($\Delta\sigma$) yielding the final estimate $\sigma_2 = \sigma_1 + \Delta\sigma$. In order to quantitatively and equitably corroborate the results from all approaches, we first normalize the reconstructions and compare them to the true crack geometries extracted from the Damage Level 4 photograph by generating a binary image using a simple thresholding technique and interpolating the assumed binary distribution (0 for a crack, 1 for the background) onto the inversion grid. To normalize the EKF and the standard TV approaches, we use the ratio of the reconstructed conductivity to the homogeneous estimate, i.e. $\sigma_N = \frac{\sigma}{\sigma_{\text{exp}}}$. For normalizing the stacked reconstruction, and because we compute the background conductivity, we use $\sigma_N = \frac{\sigma_2}{\sigma_1}$. Note that, in all cases, we have $0 < \sigma_N \leq 1.0$ because cracking can only decrease conductivity, therefore $\sigma \leq \sigma_{\text{exp}}$ and $\sigma_2 \leq \sigma_1$. As the quantitative metric to corroborate the EKF/TV/stacked reconstructions, we calculate the root mean square error (RMSE) between σ_N and the true crack geometries. The reconstructions, true crack geometries (red lines), and RMSEs are shown in Fig. 2.

The results in Fig. 2 show that the use of the EKF approach when $k < 7$ resulted in higher error (RMSE) reconstructions than the standard TV/stacked approaches. Interestingly, however, for the case where $k = 7$, the EKF regime had a lower RMSE than the standard TV approach which may indicate that when many data sets are used, EKF may out perform standard methods. Nonetheless, unlike the former reconstruction algorithms which may take hours to days to execute, the EKF regimes took between 5 seconds ($k = 3$) and 12 seconds ($k = 7$) to run. On the other hand, to compute the one image for Damage Level 4, the standard TV approach required 554 seconds and the stacked approach required 1207 seconds to reach the stopping criteria ($\frac{||\Psi_k - \Psi_{k-1}||}{||\Psi_k||} \leq 10^{-2}$). In the authors' experience, these minimization times are typical for iterative SDT problems of this size. In this case, the speed up to compute all seven images with the EKF compared to computing one with the comparative approaches is approximately a factor of 50 – 100. Moreover, the EKF regimes have favorable resolution to ERT difference regimes [3]; in contrast though, EKF retains its quantitative nature since the observation equation is not linearized at a fixed location – in particular, we

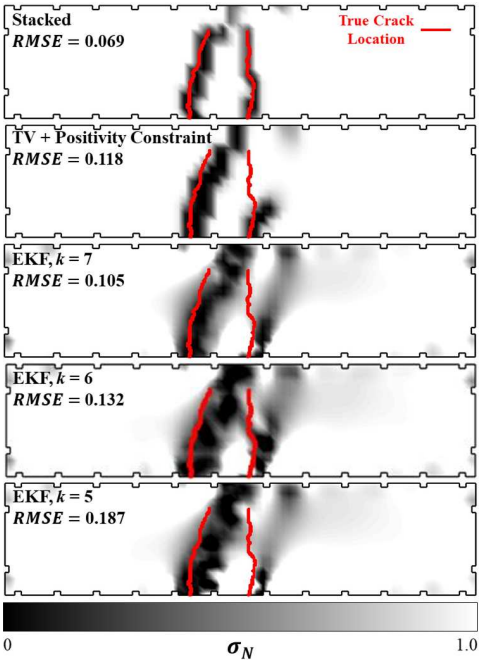

Fig. 2. Reconstructions of cracks at Damage Level 4 reporting normalized values with true crack locations plotted atop in red and the corresponding RMSEs shown on the left hand side.

refer to the fact that the sensitivity matrix is not linearized about some stationary point and the covariance matrix is non-stationary. In general, however, there is always a tradeoff between algorithm speed and spatial resolution in tomography. Nonetheless, when multiple data sets are available over a range of time, we have shown that this information can be used to quantitatively to rapidly image structural damage using state estimation.

IV. CONCLUDING REMARKS

In this work, we aimed to determine the feasibility of treating structural damage tomography as a state estimation problem. To investigate this, we applied an extended Kalman filter regime to electrical resistance tomography imaging of progressive cracking on an experimentally-tested reinforced concrete beam. Our results supported the viability of state estimation for damage tomography. By leveraging temporal data and treating the damage tomography problem as a stochastic process, it was shown that quantitative images of damage are possible with a speedup factor of approximately 50 – 100 relative to a standard TV-regularized approach and a stacked approach. It was noted, however, that the speed up was at the sacrifice of some spatial resolution.

ACKNOWLEDGEMENTS

DL was supported by the National Natural Science Foundation of China under Grant No. 61871356 and Anhui Provincial Natural Science foundation under Grant 1708085MA25.

REFERENCES

[1] D. Smyl, S. Bossuyt, W. Ahmad, A. Vavilov, and D. Liu, "An overview of 38 least squares-based frameworks for structural damage tomography," *Structural Health Monitoring*, vol. (in press), 2019.

[2] T. Tallman, S. Gungor, K. Wang, and C. Bakis, "Damage detection and conductivity evolution in carbon nanofiber epoxy via electrical impedance tomography," *Smart Mater. Struct.*, vol. 23, no. 4, pp. doi: 10.1088/0964–1726/23/4/045 034, 2014.

[3] M. Hallaji and M. Pour-Ghaz, "A new sensing skin for qualitative damage detection in concrete elements: Rapid difference imaging with electrical resistance tomography," *NDT & E INT*, vol. 68, pp. 13–21, 2014.

[4] J. Kang, Y. Ososkov, J. D. Embury, and D. S. Wilkinson, "Digital image correlation studies for microscopic strain distribution and damage in dual phase steels," *Scripta Materialia*, vol. 56, no. 11, pp. 999–1002, 2007.

[5] D. Smyl, M. Pour-Ghaz, and A. Seppänen, "Detection and reconstruction of complex structural cracking patterns with electrical imaging," *NDT&E INT*, vol. 99, pp. 123–133, 2018.

[6] H. Chai, S. Momoki, Y. Kobayashi, D. Aggelis, and T. Shiotani, "Tomographic reconstruction for concrete using attenuation of ultrasound," *NDT&E INT*, vol. 44, no. 2, pp. 206–215, 2011.

[7] L. Zhao, J. Yang, K. Wang, and F. Semperlotti, "An application of impediography to the high sensitivity and high resolution identification of structural damage," *Smart Materials and Structures*, vol. 24, no. 6, p. 065044, 2015.

[8] H. Hassan, F. Semperlotti, K.-W. Wang, and T. N. Tallman, "Enhanced imaging of piezoresistive nanocomposites through the incorporation of nonlocal conductivity changes in electrical impedance tomography," *Journal of Intelligent Material Systems and Structures*, vol. 29, no. 9, pp. 1850–1861, 2018.

[9] J. P. Kaipio, P. A. Karjalainen, E. Somersalo, and M. Vauhkonen, "State estimation in time-varying electrical impedance tomography," *Annals of the New York Academy of Sciences*, vol. 873, no. 1, pp. 430–439, 1999.

[10] A. Seppänen, M. Vauhkonen, E. Somersalo, and J. Kaipio, "State space models in process tomography—approximation of state noise covariance," *Inverse Problems in Engineering*, vol. 9, no. 5, pp. 561–585, 2001.

[11] G. Ligorio and A. M. Sabatini, "A novel kalman filter for human motion tracking with an inertial-based dynamic inclinometer," *IEEE Transactions on Biomedical Engineering*, vol. 62, no. 8, pp. 2033–2043, 2015.

[12] A. K. Khambampati, A. Rashid, U. Z. Ijaz, S. Kim, M. Soleimani, and K. Y. Kim, "Unscented kalman filter approach to tracking a moving interfacial boundary in sedimentation processes using three-dimensional electrical impedance tomography," *PHILOS T R SOC A*, vol. 367, no. 1900, pp. 3095–3120, 2009.

[13] U. Z. Ijaz, A. K. Khambampati, J. S. Lee, S. Kim, and K. Y. Kim, "Nonstationary phase boundary estimation in electrical impedance tomography using unscented kalman filter," *J. Comp. Phys.*, vol. 227, no. 15, pp. 7089–7112, 2008.

[14] D. Liu, D. Smyl, and J. Du, "Nonstationary shape estimation in electrical impedance tomography using a parametric level set-based extended kalman filter approach," *IEEE T INSTRUM MEAS*, vol. (in press), 2019.

[15] J. Yao and M. Takei, "Application of process tomography to multiphase flow measurement in industrial and biomedical fields: A review," *IEEE Sensors Journal*, vol. 17, no. 24, pp. 8196–8205, 2017.

[16] J. Zhao, M. Netto, and L. Mili, "A robust iterated extended kalman filter for power system dynamic state estimation," *IEEE Transactions on Power Systems*, vol. 32, no. 4, pp. 3205–3216, 2016.

[17] E. Wan and R. Van Der Merwe, "The unscented kalman filter for nonlinear estimation," in *Proceedings of the IEEE 2000 Adaptive Systems for Signal Processing, Communications, and Control Symposium*. IEEE, 2000, pp. 153–158.

[18] D. Bernal, "Kalman filter damage detection in the presence of changing process and measurement noise," *Mech. Sys. Sig. Proc.*, vol. 39, no. 1, pp. 361–371, 2013.

[19] M. Wu and A. W. Smyth, "Application of the unscented kalman filter for real-time nonlinear structural system identification," *Structural Control and Health Monitoring*, vol. 14, no. 7, pp. 971–990, 2007.

[20] J. N. Yang, S. Lin, H. Huang, and L. Zhou, "An adaptive extended kalman filter for structural damage identification," *Structural Control and Health Monitoring*, vol. 13, no. 4, pp. 849–867, 2006.

[21] K. Kim, B. Kim, M. Kim, Y. Lee, and M. Vauhkonen, "Image reconstruction in time-varying electrical impedance tomography based on the extended kalman filter," *Measurement Science and Technology*, vol. 12, no. 8, p. 1032, 2001.

[22] S. Liu, J. Jia, Y. D. Zhang, and Y. Yang, "Image reconstruction in electrical impedance tomography based on structure-aware sparse bayesian learning," *IEEE transactions on medical imaging*, vol. 37, no. 9, pp. 2090–2102, 2018.

[23] M. Vauhkonen, "Electrical impedance tomography and prior information," Ph.D. Thesis, University of Kuopio, Finland, 1997.

[24] Y. Wang, S. Ren, and F. Dong, "A transformation-domain image reconstruction method for open electrical impedance tomography based on conformal mapping," *IEEE Sensors Journal*, vol. 19, no. 5, pp. 1873–1883, 2018.

[25] J. Kaipio, V. Kolehmainen, M. Vauhkonen, and E. Somersalo, "Inverse problems with structural prior information," *Inverse Problems*, vol. 15, pp. 713–729, 1999.

[26] L. M. Heikkinen, T. Vilhunen, R. M. West, and M. Vauhkonen, "Simultaneous reconstruction of electrode contact impedances and internal electrical properties: Ii. laboratory experiments," *Meas. Sci. Tech.*, vol. 13, no. 12, p. 1855, 2002.